

In situ biodistribution and residency of a topical anti-inflammatory using fluorescence lifetime imaging microscopy

A. Alex,¹ S. Frey,¹ H. Angelene,² C.D. Neitzel,³ J. Li,⁴ A.J. Bower,⁴ D.R. Spillman Jr,⁴ M. Marjanovic,⁴ E.J. Chaney,⁴ J.L. Medler,³ W. Lee,³ L.S. Vasist Johnson,¹ S.A. Boppart⁴ and Z. Arp¹

¹GSK, Collegeville, PA, U.S.A.

²GSK, Bangalore, India

³Carle Foundation Hospital, Urbana, IL, U.S.A.

⁴University of Illinois at Urbana-Champaign, Urbana, IL, U.S.A.

Summary

Correspondence

Zane A. Arp.

E-mail: zane.a.arp@gsk.com

Stephen A. Boppart.

E-mail: boppart@illinois.edu

Accepted for publication

3 July 2018

Funding sources

This study was funded by GlaxoSmithKline (protocol 201661) and registered on ClinicalTrials.gov (NCT02411162). A.J.B. was supported, in part, by a National Science Foundation Graduate Research Fellowship (DGE-1144245) and a University of Illinois at Urbana-Champaign (UIUC) Electrical and Computer Engineering Distinguished Research Fellowship. J.L. was supported, in part, by the Beckman Institute Graduate Fellowship (Beckman Institute for Advanced Science and Technology) and a Support for Under-Represented Groups in Engineering (SURGE) Fellowship (UIUC).

Conflicts of interest

S.A.B. received grant support from GlaxoSmithKline related to the research described here, and reports receiving consultation fees from and owning an equity interest in PhotoniCare Inc. and Diagnostic Photonics Inc. Z.A., A.A., S.F., H.A. and L.S.V.J. are all employees and shareholders of GlaxoSmithKline.

DOI 10.1111/bjd.16992

Background GSK2894512 is a topically delivered investigational drug being developed for treatment of atopic dermatitis and psoriasis.

Objectives To investigate, in a phase I clinical trial, the spatial biodistribution and residency of GSK2894512 within the epidermis and dermis of healthy human participants noninvasively using fluorescence lifetime imaging microscopy (FLIM).

Methods Two topical drug formulations containing GSK2894512 1% were applied to the right and left forearms of six participants for seven consecutive days, followed by seven days of observation for residency. FLIM images were obtained daily throughout the study, approximately every 24 h. During the treatment phase of the study, images were collected from each participant pretreatment, reflecting the residual dose from the previous day. Three punch biopsies from each participant of one formulation was obtained from the treated region during the post-treatment follow-up period between days 8 and 14 for comparison with FLIM results.

Results Cellular and subcellular features associated with different epidermal and dermal layers were visualized noninvasively, down to a depth of 200 µm. Results yielded three-dimensional maps of GSK2894512 spatial distribution and residency over time. This fluorescence data provided a marker that was used as a monitor for day-to-day variance of drug presence and residency postapplication.

Conclusions The results suggest FLIM could be a viable alternative to skin biopsies without the usual patient discomfort and limitations, thereby enabling the direct measurement of skin distribution through longitudinal monitoring. These results are the first step in establishing the unique capabilities that multiphoton imaging could provide to patients through noninvasive drug detection.

What's already known about this topic?

- Fluorescence lifetime imaging (FLIM) has been used to image noninvasively cellular features in humans.
- FLIM has demonstrated the potential to monitor morphological and metabolic changes at the subcellular level that occur in patients with skin cancer and atopic dermatitis.
- Its potential for wider utilization in dermal drug discovery or dermatological disease monitoring has seen limited development.

What does this study add?

- This is a first-of-its-kind clinical study in which FLIM was used to monitor drug distribution and residency.
- It is a first step in establishing the unique capabilities multiphoton imaging could provide to patients via noninvasive drug detection.
- More information was generated per patient while reducing patient burden and population size using FLIM.
- Imaging end points can be utilized to improve patient outcomes through improved monitoring capabilities.

What is the translational message?

- Optical imaging can assess the heterogeneity of pharmacokinetic responses to topical drugs with optical signatures.
- Advanced nonlinear optical imaging techniques can provide label-free contrast in skin, which allows investigation of the efficacy of a topical treatment by monitoring structural/functional changes in skin.
- Personalized therapeutic approaches may be possible by visualizing the distribution, residency and clearance of anti-inflammatory drugs.
- Commercial imaging systems facilitate the translation of nonlinear optical imaging techniques into clinical applications.

Understanding penetration characteristics of the active pharmaceutical ingredient (API) in topical formulations such as volumetric dispersion, penetration and residency are necessary for successful treatment of dermatological conditions. To gain this understanding, a variety of different methods can be utilized to investigate penetration and biodistribution within skin, either *ex vivo* or *in vivo*. An overview of many of these methods can be found in the Supporting Information (Appendix S1), along with limitations of these techniques that could be addressed by advanced imaging methods. Owing to these limitations, an imaging technique that can provide label-free mapping of spatial distribution, penetration pathways and residency of topical formulation on skin *in vivo* will be an extremely valuable tool for topical formulation development and monitoring disease outcomes.

The purpose of this article is to report results of a phase I clinical trial of a topically delivered investigational drug, GSK2894512,¹ a drug being developed for treatment of atopic dermatitis and psoriasis, in healthy participants, using interpreted results from fluorescence lifetime imaging microscopy (FLIM) as the primary end point. Multiphoton FLIM is a relatively new noninvasive optical imaging technique that measures fluorescence lifetimes of fluorophores to generate image contrast and can be used to monitor metabolic, chemical and morphological changes *in vivo*.^{2,3} Although excitation and emission wavelengths of bound and unbound nicotinamide adenine dinucleotide (phosphate) NAD(P)H are the same, fluorescence lifetimes of NAD(P)H in each state are significantly different, with unbound being ~0.4 ns and bound being ~2 ns. This differentiation can be utilized as a marker for

metabolic activity.⁴ In a previous study investigating the transdermal kinetics of a drug formulation in human skin sections *ex vivo*, FLIM was used to monitor the drug's diffusion pathway by measuring the variation in bound NAD(P)H fluorescence lifetime before and 2 h after drug application.⁵ In addition to NAD(P)H, a variety of additional endogenous fluorophores are also observed in skin.^{6–8} These characteristics makes FLIM a promising technique for label-free skin imaging.

In this clinical study of healthy participants, penetration, spatial distribution and residency of two topical formulations of GSK2894512 (cream A and cream B) were evaluated longitudinally using FLIM. This drug exhibits inherent fluorescence properties (lifetime ~3000 ps), which allows differentiation from endogenous fluorescent components in human skin. By using the fluorescent properties of GSK2894512, the penetration kinetics of this drug were followed in six healthy participants for both formulations daily throughout a 14-day residency study. To our knowledge, this is a first-of-its kind clinical study in which FLIM was used to monitor drug distribution and residency in a clinical setting, and is the first step in establishing the unique capabilities that this type of imaging provides to follow drug effects noninvasively on patient outcomes in a clinical setting.

Materials and methods

Study participants and topical treatment

Seven healthy white men (Fitzpatrick skin type I–IV) aged 18–32 years were enrolled in this phase I clinical trial during a 3-month period (July–September 2015). Six participants

completed the study; one withdrew consent on day 6. Each participant received 3 mg cm⁻² 1% concentration of each study cream. Cream A was applied to one volar forearm and cream B was applied to the other volar forearm once daily for 7 days. To monitor background fluorescence in FLIM, vehicle creams were imaged on day 1 in a separate area of the forearm (at least 1.3 cm from where study drug was applied).

The human subject research component was approved by the Carle Foundation Hospital Institutional Review Board. Informed consent was obtained from healthy participants prior to any study procedures.

Fluorescence lifetime imaging microscopy

The study participants were comfortably seated on a recliner chair with armrests and the volar forearm of the subject was securely positioned on the armrest with cushion support, which helped to reduce the motion artefacts during the imaging session. Prior to imaging, using double-sided tape, a glass coverslip was placed on a magnetic coupling ring, which was then attached to the volar forearm imaging site. Subsequently, the articulated arm of the imaging system was attached to the magnetic coupling ring (Fig. 1e). A CE-certified multimodal optical imaging system (MPTflex™ CARS; JenLab, Jena, Germany) was used to acquire FLIM images *in vivo*. FLIM images were obtained from study participants from day 1 to day 15, including control images on day 1 (prior to initial drug

application). To generate FLIM images, the excitation wavelength of the femtosecond laser was set to 725 nm and *in situ* laser power was set to 30 mW – well below ANSI Z136.1 (2014) safety limits. Two sets of volumetric FLIM datasets corresponding to 200 µm × 200 µm × 200 µm volumes were acquired from within the 7 cm × 14 cm treatment region per study day. FLIM images were taken in 5-µm steps from the skin surface down to a depth of 200 µm, with spatial resolutions of < 0.5 µm horizontally and < 2 µm vertically. The time required to acquire each volumetric FLIM dataset was approximately 8 min.

The details of the detection part of this multimodal imaging system have been described previously.⁹ The imaging system comprised of four different detection channels where the autofluorescence signal was collected by the first detection channel (405–565 nm) and the vast majority of drug fluorescence signal was detected by the second channel (370–405 nm). As most of the drug signal was detected in the second channel (Figs S1 and S2; see Supporting Information), only the signal collected in this channel was analysed to determine the drug distribution and residency from the FLIM images.

Fluorescence lifetime imaging microscopy analysis

Fluorescence decay data from FLIM images were processed offline using commercial software, SPCImage (Becker and

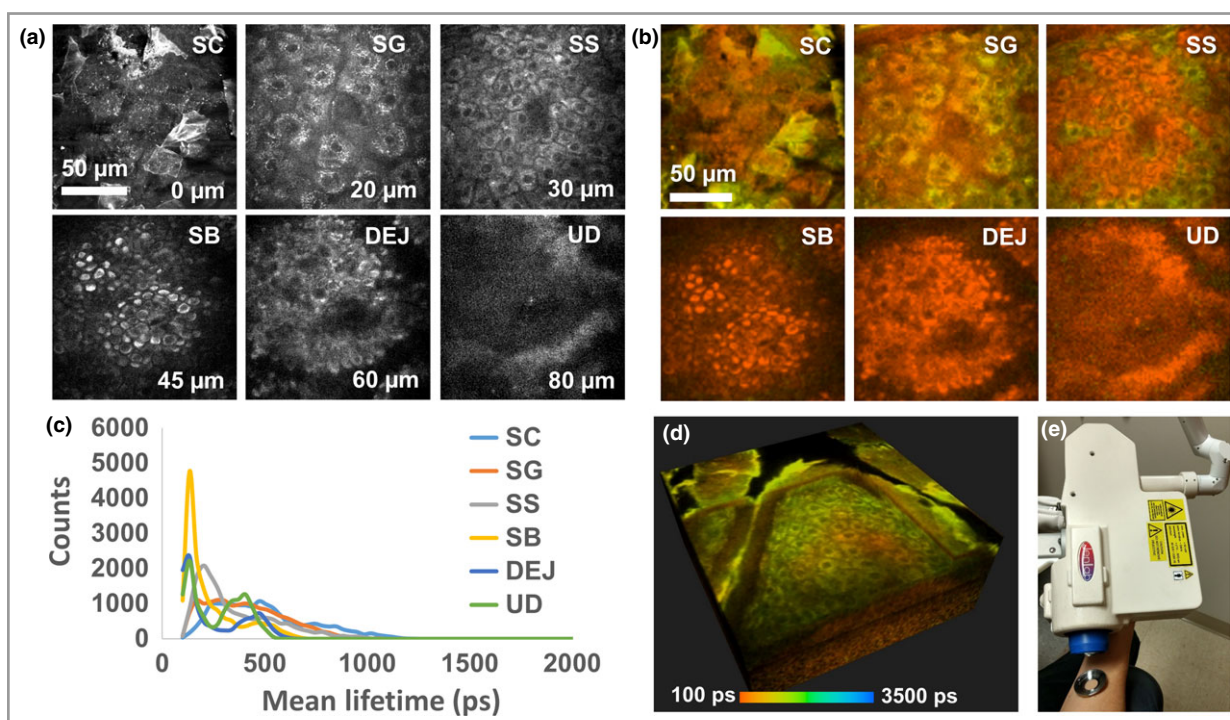


Fig 1. Optical imaging of human skin *in vivo*. (a) Two-photon excited fluorescence images of different skin layers. (b) Fluorescence lifetime imaging microscopy (FLIM) images of different skin layers. (c) Mean lifetime distribution in different skin layers. (d) Three-dimensional rendering of skin from FLIM images and (e) coupling tomography head to skin for *in vivo* imaging. SC, stratum corneum; SG, stratum granulosum; SS, stratum spinosum; SB, stratum basale; DEJ, dermal–epidermal junction; UD, upper dermis.

Hickl, Berlin, Germany). Fluorescence decay curves obtained from each pixel of the FLIM dataset were fitted using a standard multiparameter exponential decay, the full details of which can be found in the Supporting Information (Appendix S2). From the fitting, three variables were used to discriminate endogenous fluorescence from the study drug: mean lifetime (τ_m); second lifetime component (τ_2) from a two-component fit; and absolute third fractional component (a_3) from a three-component fit. Typically, endogenous fluorophores in healthy skin have $\tau_m < 2200$ ps, $\tau_2 < 3500$ ps and no appreciable a_3 component.¹⁰ These variables were selected based on literature evidence,^{10,11} and experimentally confirmed by comparing FLIM images from control regions (day 1 and vehicle cream images) with those obtained from the treatment regions. Fluorescence signal attributed to GSK2894512 from each pixel was determined using an analysis algorithm (Fig. 2). Total drug fluorescence was quantified by integrating drug fluorescence measured from all pixels within a full volumetric dataset using a custom-written MATLAB algorithm (MathWorks, Natick, MA, U.S.A.).

Liquid chromatography–tandem mass spectrometry analysis

GSK2894512 was extracted from human skin tissue homogenate by protein precipitation, using acetonitrile containing [2H₂13C₆]-GSK2894512 as an internal standard. Extracts were analysed by high-performance liquid chromatography tandem mass spectrometry (LC–MS/MS) using a TurboIonSpray™ interface with negative ion multiple reaction monitoring. This method was validated over the range 0.5–1000 ng mL⁻¹ and the lower limit of quantification (LLQ) was 0.5 ng mL⁻¹ using a 50- μ L aliquot of human tissue homogenate. Concentrations of GSK2894512 were normalized to ng mg⁻¹ skin tissue.

Results

Optical biopsy of human skin

FLIM allows noninvasive visualization of the microstructural organization and biochemical composition of human skin *in situ*. Endogenous fluorophores in human skin such as NAD(P)H,

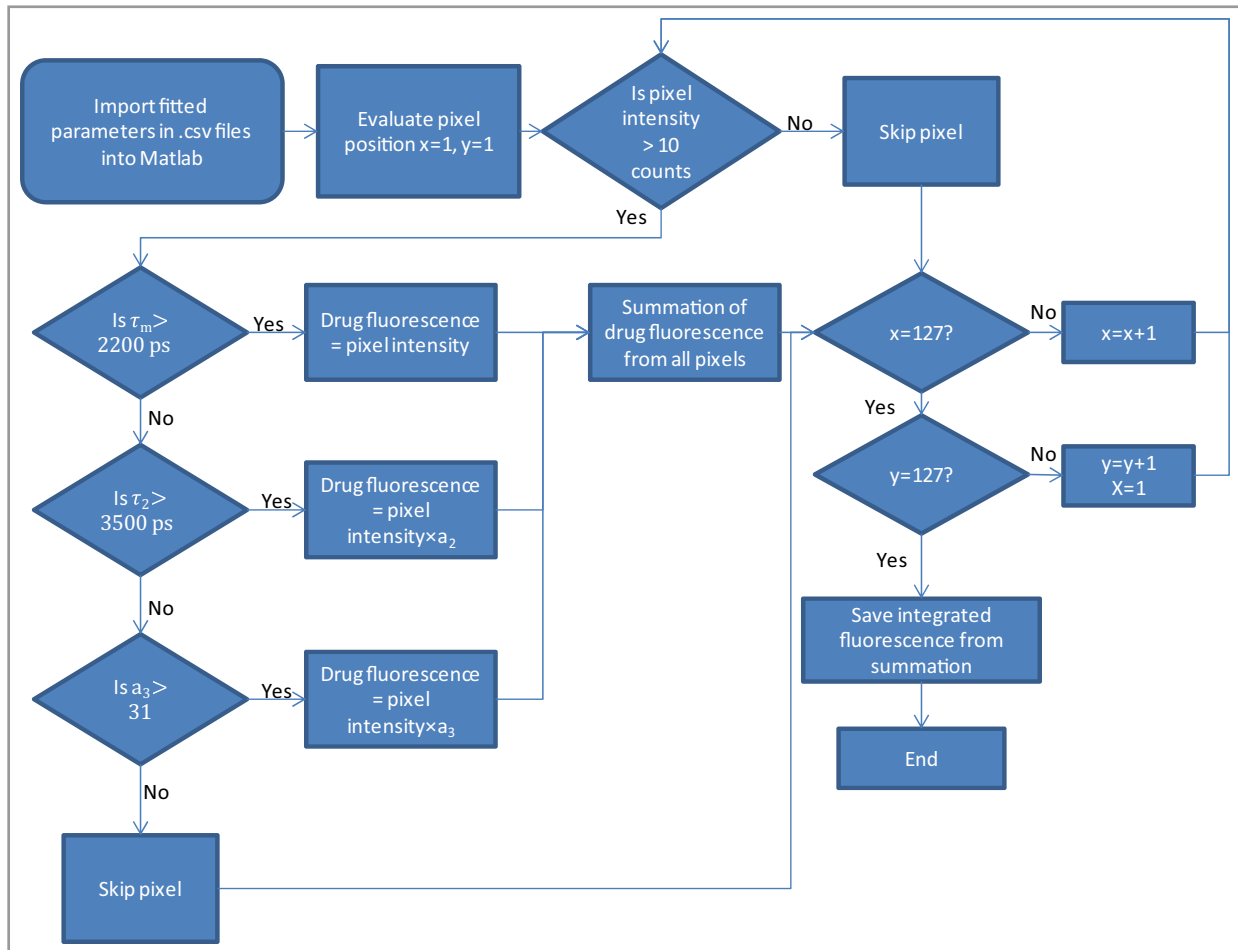


Fig 2. Flowchart of fluorescence lifetime imaging microscopy (FLIM) data analysis. Raw FLIM data were analysed with SPCImage software (Becker and Hickl, Berlin, Germany). Output parameters such as τ_m , τ_2 , τ_3 , a_3 (abs), a_3 (%) and pixel intensities were imported to Matlab for further analysis. Each FLIM image comprised 127×127 pixels with 40 frames per volumetric dataset. In MATLAB, images are analysed pixel by pixel, as shown in the flowchart, to determine the spatial distribution and contribution of drug to the measured fluorescence signal.

flavins, porphyrins, elastin, keratin and melanin enable label-free visualization of cellular and subcellular details of different skin layers *in vivo*.^{6–8} In comparison to confocal microscopy, two-photon excited fluorescence provides superior spatial resolutions and deeper penetration, up to ~200 µm in scattering tissues. As shown in Figure 1(a), different sublayers of epidermis, such as stratum corneum (SC), stratum granulosum (SG), stratum spinosum (SS) and stratum basale (SB), can be differentiated based on cellular features in those layers. As shown in previous studies,³ fluorescence lifetime depends on the chemical composition of that region and is an indicator of its metabolic state. Figure 1(b) shows FLIM images of different skin layers and Figure 1(c) shows histograms of mean fluorescence lifetime at corresponding depths. As melanin has a lower fluorescence lifetime than keratin, melanocytes and keratinocytes can be easily distinguished from surrounding tissue in FLIM images. A three-dimensional (3D) rendering of the imaged volume of human skin reconstructed from FLIM images demonstrates the 'optical biopsy' capabilities of these imaging modalities (Fig. 1d).

Mapping and quantification of three-dimensional biodistribution of the topical creams *in vivo*

Fluorescence signal from the topical cream was discriminated from endogenous fluorescence based on its longer fluorescence lifetime. FLIM images were colour-coded according to fluorescence lifetime, where regions with a mean fluorescence lifetime (τ_m) > 3500 ps are presented in blue. Figure 3(a) shows penetration of the topical cream along a hair follicle. These FLIM images were obtained 24 h postapplication and showed that most of the topical cream remained in the SC layer and accumulated along ridges of the skin. A 3D rendering depicting penetration of the topical cream along the hair follicle is shown in Figure 3(b). Depth of penetration of the topical cream was determined from these depth-resolved FLIM images (Fig. 3c). Using these approaches, it was also possible to detect both stronger signals from concentrated drug and weaker signals from dispersed drug (Figs S3–S5; see Supporting Information). In addition to the fluorescence decay-fitting technique, the differentiation of the drug fluorescence signal from endogenous fluorescence was confirmed using phasor analysis, and drug biodistributions estimated using both analysis approaches were similar (Fig. S6; see Supporting Information).

Determining skin residency of a topical cream

Two different formulations of the same API were applied on the volar forearm of participants for seven consecutive days and FLIM images were obtained from treated regions 24 h after application (control images were obtained on day 1 prior to application). To determine the skin residency of the topical cream, FLIM images were taken daily throughout the study. Spatial distribution, depth of penetration and residency of the topical formulation were determined based on the FLIM images. Figure 4 depicts FLIM images from one study participant, demarcating drug signal (shown as blue regions) at different depths on different days of this longitudinal study. Optimal

parameters for discriminating drug signal were determined experimentally by analysing control images from predose on day 1 and vehicle control images obtained 24 h post-dose from day 1 application. On treatment days 2–7, most of the drug signal was detected on the skin surface (Fig. 4c, d). Accumulation of the topical formulation along skin ridges is also visible in images obtained on days 2, 8 and 9 (Fig. 4 i, j, k, p). By day 10, there was no detectable fluorescence from formulation residing in the skin (Fig. 4f, l, r). Figure 4 shows results from one participant with inter-participant variability large in terms of amount of drug present on skin and its residency (Figs S7 and S8; see Supporting Information).

Fluorescence lifetime imaging microscopy clinical readouts

Drug fluorescence detected using FLIM from different skin layers for both creams were semi-quantified. Figure 5(a, b) shows drug fluorescence signal, depth of penetration and residency in one study participant for cream A and B. In this participant, fluorescence signal from both formulations were detected above limits of detection on all treatment days, except on day 4 for cream A (Fig. 5a). However, no appreciable amount of drug fluorescence was detected from either cream during the post-treatment period (i.e. after day 8).

Figure 6(a) shows average depth-integrated fluorescence signals from both creams on different days of the study ($n = 6$). Large day-to-day variations were observed in fluorescence signal for both creams during the treatment period, with maximum fluorescence signal observed on day 7 for cream A and on day 6 for cream B. For both creams, an average drug fluorescence was not observable below 60 µm (Fig. 6b). During the post-treatment period, fluorescence from the drug was detected above the detection threshold 48 h post-dose (day 9) for cream A and 24 h post-dose (day 8) for cream B.

Punch biopsies (4 mm) were taken from the cream B-treated region from all participants on day 8. Participants were randomized to have two more biopsies collected between days 9 and 14. Biopsies from cream A were not taken, as confidence in the ability to observe its behaviour with FLIM was high based on the drug's optical characteristics, allowing the trial to be reduced from 12 patients to six, thus reducing participant burden. Biopsies were analysed using LC–MS/MS to characterize pharmacokinetic properties of the drug. Bioanalytical results indicated that there was a mean \pm SEM of 172.5 ± 46.132 ng drug g^{-1} tissue present in the skin 24 h after last application (day 8, $n = 6$), and 20.9 ± 20.937 ng g^{-1} present 48 h after last application (day 9, $n = 2$), with the LLQ being approximately 25 ng per gram of tissue (Fig. 6c). The LC–MS/MS results of cream B showed a similar trend to the results obtained using FLIM during this time period.

Discussion

In this study, two formulations (cream A and cream B) of the topical drug GSK2894512 were investigated to detect their

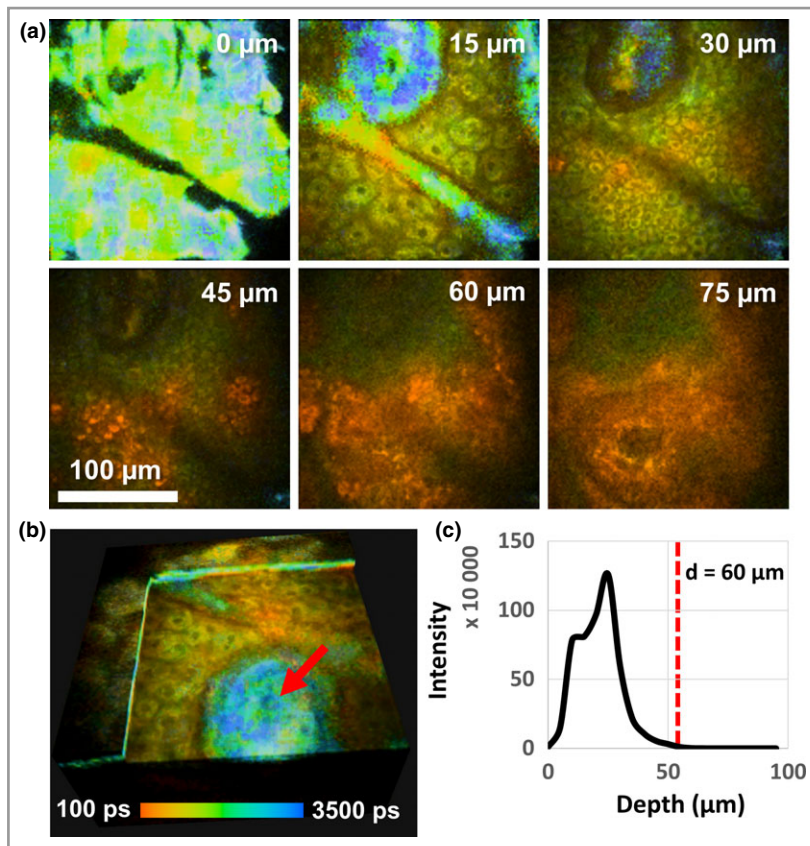


Fig 3. Drug penetration into skin through a hair follicle. (a) Fluorescence lifetime imaging microscopy (FLIM) images acquired from a region treated with cream B 24 h post-dose. These FLIM images are obtained from different skin layers, whose corresponding depths below the skin surface are denoted on the images. The blue regions are pixels with a fluorescence lifetime > 3500 ps, which corresponds to the fluorescence signal from drug. The extent of drug penetration and penetration pathways are visible in these FLIM images. (b) A three-dimensional rendering of the volumetric FLIM dataset obtained from the same region, depicting the drug penetration through the hair follicle (red arrow). (c) Estimation of the drug penetration depth by quantifying the drug fluorescence at different depths. In this representative FLIM dataset, penetration depth was determined to be $60 \mu\text{m}$ (denoted by red dashed line).

penetration and residency in healthy participants. GSK2894512 has inherent fluorescent properties and a long fluorescence lifetime, which enabled its detection from endogenous fluorescence signal using FLIM *in situ*. The noninvasive nature of the method significantly increased the amount of information that could be generated per participant, while simultaneously reducing participant burden. Penetration and residency of both formulations of GSK2894512 were imaged in all six participants daily (in duplicate) through vehicle control, treatment and postapplication phases of the study, whereas biopsies were only collected from participants during the postapplication phase of the study from one formulation. To achieve a similar evaluation of these formulations penetration and residency using only traditional methods would have required biopsies for each day from six participants for both tested formulations in all phases of the study. This would have required 180 physical biopsies to be collected. In this study, a maximum of three biopsies were allowed per participant, which would have required at least 60 participants to perform a similar study using biopsies. These calculations are based on a single data point per participant. Twice as many participants

and biopsies would be have been needed to achieve comparable information as was acquired through FLIM, as it was taken in duplicate. In using FLIM, a significant reduction in clinical trial size is achievable, reducing overall trial costs, participant burden and likelihood of complications from biopsy.

There was significant variation in the day-to-day observation of drug fluorescence from both formulations throughout the treatment phase of this study as shown by FLIM. This is an interesting finding as the drug was applied on a daily basis by clinicians, to ensure compliance with drug delivery. Additionally, participants were required to refrain from activities that would remove the drug, such as showering, strenuous activity for the first 4 h post-dose, swimming and use of hot tubs for the duration of the study. From a clinical perspective, this type of variation could have important implications on establishing a dosing schedule, because significant variation in drug presence on skin reduces the efficacy of the formulation, regardless of the drug. Because both formulations indicated this variation, it is likely that there are factors, outside controls within the protocol, influencing retention of the drug. For topical treatments, it is important to understand and limit, or

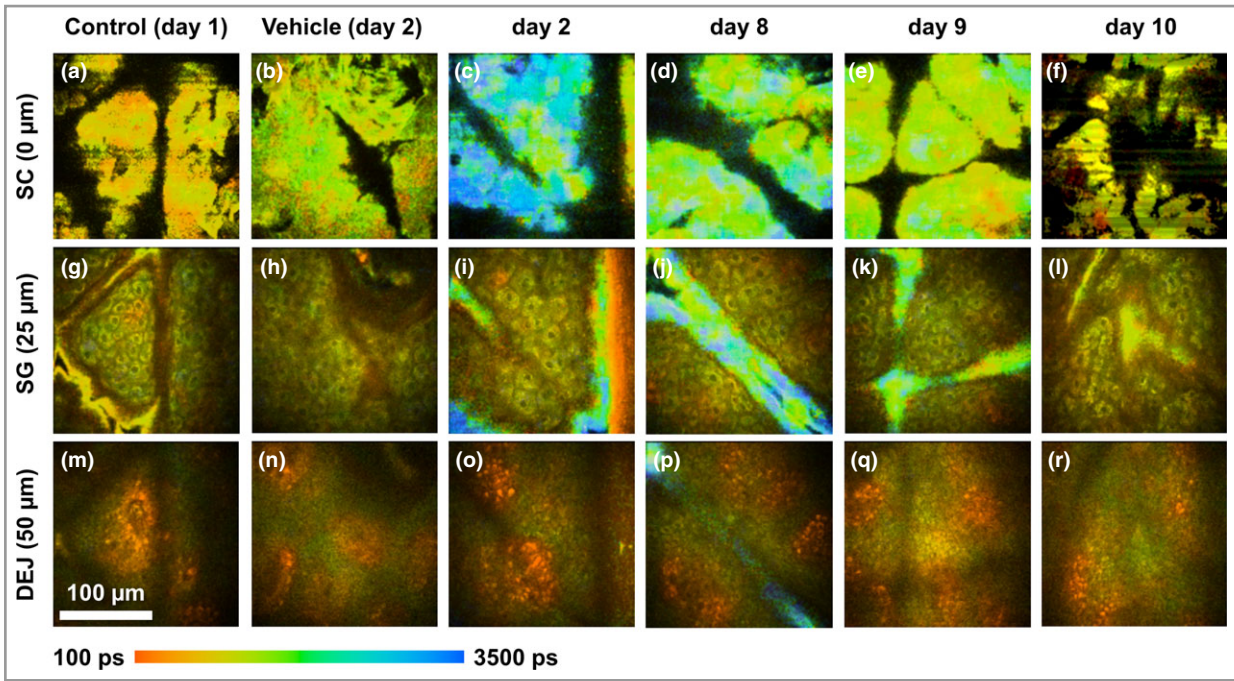


Fig 4. Longitudinal fluorescence lifetime imaging microscopy (FLIM) images showing distribution of cream A in different skin layers on different days of the study: (a–f) stratum corneum (SC), (g–l) stratum granulosum (SG) and (m–r) dermal–epidermal junction (DEJ). All blue regions indicate fluorescence signal from the drug. Each row represents images taken from different depths (0 μm, 25 μm and 50 μm).

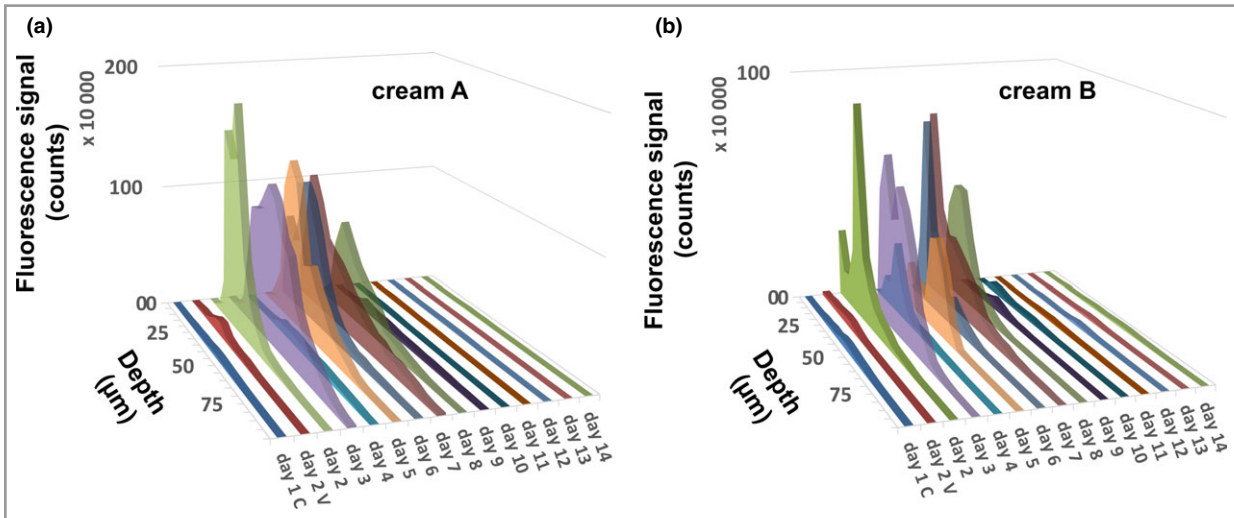


Fig 5. Determining depth of penetration and skin residency of the topical formulations using fluorescence lifetime imaging microscopy (FLIM). Representative plots showing the fluorescence signal quantified from different depth sections of a healthy participant on different days of the study for (a) cream A and (b) cream B. Day 1 C and day 2 V represent measurements from control images obtained before treatment on day 1 and from vehicle images on day 2, respectively. Days 1–7 are treatment days and FLIM images were obtained until day 14.

compensate, for these variations to ensure best patient outcomes.

The post-application phase of this study was followed by both FLIM and bioanalysis of biopsies from cream B. Bioanalytical results showed detectable drug on day 8, significantly less drug on day 9 and below limit of detection of drug on days 10–14. Although quantitative concentrations of drug

were not measured with FLIM, bioanalytical results compare well with fluorescence signal monitored by FLIM. Owing to the small number of participants and limitations in biopsy collection, the FLIM results cannot be completely validated by bioanalytical analysis from this study alone. A significant drug presence was still seen with FLIM 24 h after the last dose (day 8), and only minor quantities present at 48 h after the last

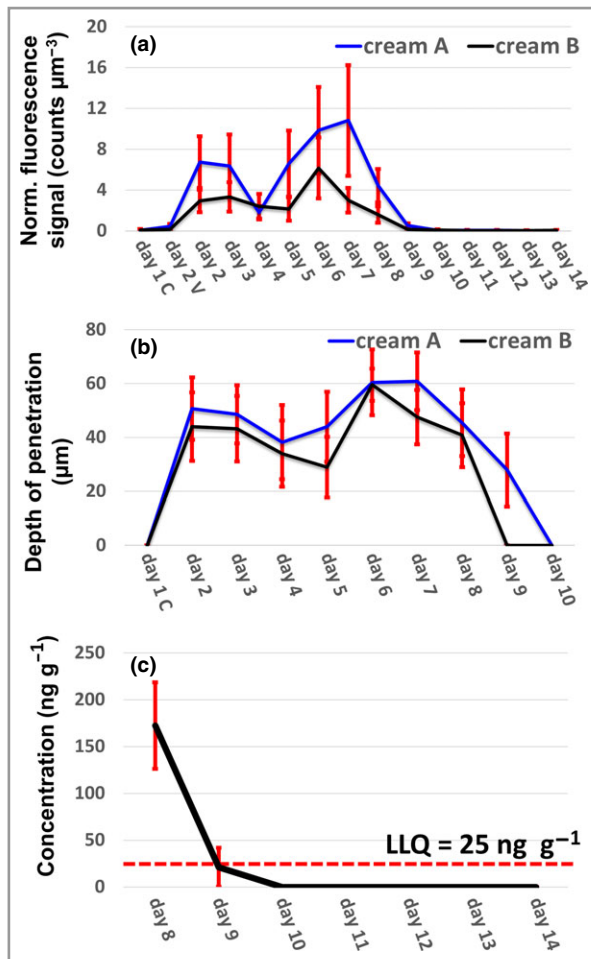


Fig 6. Combined readout of (a) skin residency and (b) depth of penetration determined by analysis of fluorescence lifetime imaging microscopy (FLIM) images for creams A and B ($n = 6$). (c) Pharmacokinetic concentration–time plot for cream B obtained from biopsy samples using liquid chromatography–mass spectrometry/mass spectrometry (LC–MS/MS). The lower limit of quantification (LLQ) of the assay was 25 ng g^{-1} . Day 1 C and day 2 V represent measurements from control images obtained before treatment on day 1 and from vehicle images on day 2, respectively. Days 1–7 are treatment days and FLIM images were obtained until day 14. Biopsies for LC–MS/MS measurements were taken during the post-treatment period (days 8–14). The results in the subplots are presented as mean \pm SEM.

dose (day 9). As spatial information was also observed with FLIM, it was possible to observe the spatial distribution of GSK2894512. The minor quantities of drug present were largely found in the furrows of the skin and not in its deeper layers. This type of spatial information would not have been visible using traditional bioanalytical methods.

It is worth noting that the absence of fluorescent signal may not necessarily mean lack of significant picomolar quantities of drug presence, which may still be exerting an effect in the dermis. Owing to the scattering of emitted fluorescent light in dense tissues such as skin, there can be limitations on the sensitivity of noninvasive optical imaging techniques such as FLIM to

detect small quantities of drug in deeper regions. However, the lack of observation of drug in the skin by LC–MS/MS gives confidence that these smaller drug quantities are probably not present. Moreover, metabolism or ligand engagement of the drug could alter the fluorescent properties of the drug such that they are not detectable with this method. Another aspect to consider is the likelihood of photo-bleaching, which may occur during the imaging, and should be accounted for when quantifying the drug fluorescence signal. With these limitations in mind, we suggest that the majority of the FLIM signal for both formulations was dispersed in the SC, skin furrows and in hair follicles. This important finding helps to improve our understanding of the importance of the SC/SG barrier, and to establish where within the skin the drug is getting dispersed. There were only limited differences in dispersion of the drug between the two formulations in this study.

In conclusion, this exploratory study demonstrated the capability of FLIM as a novel, noninvasive imaging method to follow *in vivo* the distribution and residency of a topical medication, GSK2894512, in healthy skin. It was possible to localize the fluorescence signal of the drug emerging from different layers of skin in a label-free manner, which enabled observation of 3D biodistribution and depth of penetration of two topical formulations *in situ*. The results obtained show the several advantages offered by FLIM over current practices in topical drug development. In addition to allowing longitudinal monitoring of the same treatment region without any patient discomfort or sampling limitations, use of imaging end points can decrease the workload involved in tissue analysis, provide information on the safety and optimal dosing of test formulations, and thus improve the efficiency of the drug development process. More importantly, imaging tools such as FLIM might provide biomarkers of a disease process and much earlier surrogate markers of treatment success. Besides cellular morphological details, FLIM also provides information related to biochemical compositions of the target site, which was not utilized in this study. The variations in fluorescence lifetime can be related to metabolic changes happening in drug-treated regions. Hence, besides quantifying drug fluorescence distribution and penetration, FLIM can also be utilized to monitor pharmacodynamic changes in different skin layers and cells following topical treatment. We have shown that FLIM is a promising imaging tool that can be used for studying the pharmacokinetic properties of a topical cream *in vivo*, accelerating drug development processes, reducing costs and developing more effective and appropriate methods to perform post-treatment monitoring.

Acknowledgments

All authors meet the criteria for authorship set forth by the International Committee for Medical Journal Editors. The authors acknowledge the support of clinical staff in the Carle Department of Dermatology for their assistance in this study. The authors would also like to acknowledge Elizabeth K. Hussey, Pharm.D. for her contributions in study initiation and

design, and Kelly Gallagher of GlaxoSmithKline for manuscript preparation, collecting author comments and editing.

References

- 1 Smith SH, Jayawickreme C, Rickard DJ *et al.* Tapinarof is a natural AhR agonist that resolves skin inflammation in mice and humans. *J Invest Dermatol* 2017; **137**:2110–19.
- 2 Zhao Y, Graf BW, Chaney EJ *et al.* Integrated multimodal optical microscopy for structural and functional imaging of engineered and natural skin. *J Biophotonics* 2012; **5**:437–48.
- 3 Becker W. Fluorescence lifetime imaging – techniques and applications. *J Microsc* 2012; **247**:119–36.
- 4 Bower AJ, Arp Z, Zhao Y *et al.* Longitudinal *in vivo* tracking of adverse effects following topical steroid treatment. *Exp Dermatol* 2016; **25**:362–7.
- 5 Bird DK, Schneider AL, Watkinson AC *et al.* Navigating transdermal diffusion with multiphoton fluorescence lifetime imaging. *J Microsc* 2008; **230**:61–9.
- 6 Masters BR, So PT, Gratton E. Multiphoton excitation fluorescence microscopy and spectroscopy of *in vivo* human skin. *Biophys J* 1997; **72**:2405–12.
- 7 König K, Raphael AP, Lin L *et al.* Applications of multiphoton tomographs and femtosecond laser nanoprocessing microscopes in drug delivery research. *Adv Drug Deliv Rev* 2011; **63**:388–404.
- 8 Liang X, Graf BW, Boppart SA. *In vivo* multiphoton microscopy for investigating biomechanical properties of human skin. *Cell Mol Bioeng* 2011; **4**:231–8.
- 9 Weinigel M, Breunig HG, Uchugonova A *et al.* Multipurpose non-linear optical imaging system for *in vivo* and *ex vivo* multimodal histology. *J Med Imaging* 2015; **2**:016003.
- 10 Sanchez WY, Pastore M, Haridass IN *et al.* Fluorescence lifetime imaging of the skin. In: *Advanced Time-Correlated Single Photon Counting Applications*. (Becker W, ed.). Cham: Springer International Publishing, 2015; 457–508.
- 11 Skala MC, Riching KM, Bird DK *et al.* *In vivo* multiphoton fluorescence lifetime imaging of protein-bound and free nicotinamide adenine dinucleotide in normal and precancerous epithelia. *J Biomed Opt* 2007; **12**:024014.

Supporting Information

Additional Supporting Information may be found in the online version of this article at the publisher's website:

Appendix S1. Other methods for biodistribution monitoring.

Appendix S2. Fluorescence lifetime imaging microscopy analysis optimization.

Fig S1. Fluorescence emission spectra of creams A and B, and fluorescence lifetime imaging microscopy image of drug formulations.

Fig S2. Fluorescence signal detected on channel 1 and channel 2 of the imaging system on day 1 (control) and day 2 (cream A) from the stratum corneum layer of skin.

Fig S3. Fluorescence lifetime estimation using two-component fitting in Becker and Hickl software.

Fig S4. Discrimination of drug fluorescence signal using the constrained three-component fitting approach using a threshold criteria of $a3(abs) > 31$.

Fig S5. Illustration of drug fluorescence quantification from fluorescence lifetime imaging microscopy images based on three different analysis criteria.

Fig S6. Validation of drug distribution with phasor analysis.

Fig S7. Quantification of fluorescence signal from cream A showing depth of penetration and residency of the topical formulation on different participants.

Fig S8. Quantification of fluorescence signal from cream B showing depth of penetration and residency of the topical formulation on different participants.

Table S1. Fluorescence lifetime imaging microscopy image analysis settings used for the two- and three-component fitting in SPCImage analysis software (Becker and Hickl, Berlin, Germany).